Electronic Supplementary Material (ESI) for Journal of Materials Chemistry A.

Supporting Information

Branched Polymer-incorporated Multilayered Heterostructured Photoanode: Precisely Tuning Directional Charge Transfer Toward Solar Water Oxidation

Zhi-Quan Wei, Xiao-Cheng Dai, Shuo Hou, Yu-Bing Li, Ming-Hui Huang, Tao Li, Shuai Xu, Fang-Xing Xiao*

College of Materials Science and Engineering, Fuzhou University, New Campus, Minhou, Fujian Province 350108, China.

E-mail: fxxiao@fzu.edu.cn

Table of contents

Page NO.

Experimental Section

1. Materials

Titanium sheet (50 mm × 20 mm × 0.1 mm, 99.9%), Deionized water (DI H_2O, Millipore, 18.2 MΩ·cm resistivity), Graphite sheet (50 mm × 20 mm × 0.1 mm, 99.6%), Ethylene glycerol $(CH_2OH)_2$, Ammonium fluoride (NH_4F), Hydrogen fluoride (HF), Nitric acid (HNO_3), Sodium molybdate dehydrate ($Na_2MoO_4\cdot 2H_2O$), Dibenzyl disulfide ($C_{14}H_{14}S_2$), Ethanol (CH_3CH_2OH), Branched polyethylenimine (BPEI, average M_w=25 kDa, Sigma-Aldrich), Poly (diallyldimethylammonium chloride) solution (PDDA, average M_w=200~350 kDa, Sigma-Aldrich), Poly (allylamine hydrochloride) (PAH, average M_w=17.5 kDa, Sigma-Aldrich), Poly (sodium 4-styrenesulfonate) (PSS, average M_w=70 kDa, Sigma-Aldrich). All the chemicals are analytic grade and used as received without further purification.

2. Preparation of TNTAs substrate

Ti foil was first thoroughly sonicated in acetone, ethanol and DI H_2O for 15 min, respectively. Then, Ti sheets were immersed in a mixed solution of HF-HNO_3-H_2O with volume ratio of 1 : 4 : 5 for 20 s, washed by DI H_2O and dried with a gentle N_2 stream. Anodization was carried out under ambient conditions at 50 V for 2 h with ca. 3 cm separation distance between the working (Ti foil) and counter electrode (graphite). The electrolyte consists of 0.3 wt % of NH_4F (0.6 g) in ethylene glycol (196 mL) and DI H_2O (4 mL). After the first-step anodization, the as-obtained TiO_2 layer was removed from Ti foil by sonication in ethanol for 5 min, washed by DI H_2O and dried with a N_2 stream. The second anodization was performed at 50 V for 30 min to produce the TNTAs. Similarly, the resulting TNTAs were also washed by DI H_2O, dried with a N_2 stream and finally calcined at 450 ^oC for 3 h in air with a heating rate of 5 ^oC min^{-1}.

3. Preparation of MoS_2 quantum dots (QDs)

In brief, 0.4 g of $Na_2MoO_4\cdot 2H_2O$ was dissolved in 30 mL of DI H_2O with ultrasonication for 20 min. Then, 0.38 g of dibenzyl disulfide and 30 mL of ethanol were added to the solution followed by ultrasonication for 30 min. The mixture was then transferred into a 100 mL Teflon-line stainless steel autoclave and maintained at 220 ^oC for 18 h. Upon cooling naturally to room temperature, mother liquor was drained and new DI H_2O was added into the autoclave. The resulting suspension was then centrifuged for 60 min at 12 000 rpm to separate the supernatant and centrifugate. The light brown supernatant was MoS_2 QDs and the centrifugate was the composition of MoS_2 QDs and micro-sized particles.

4. Preparation of TB_2 and TM_2 photoanodes

TNTAs substrate was directly dipped into BPEI (0.5 mg/mL, 0.5 M NaCl, pH=10) or MoS_2 QDs aqueous solution (25 mg/L) for 1 min and then washed with DI H_2O for 1 min and dried with a stream of N_2. Based on which, TB_2 or TM_2 heterostructure can thus be fabricated by repeating the above procedure.

5. Preparation of $T(BM)_2$ photoanodes with different deposition time

TNTAs substrate was firstly dipped into positively charged BPEI aqueous solution (0.5 mg/mL, 0.5 M NaCl, pH=10) for 5 (or 1 min), washed with DI H_2O for 1 min and dried with a stream of N_2. Subsequently, BPEI-modified TNTAs was dipped into negatively charged MoS_2 QDs aqueous solution (25 mg/L) for 5 (or 1 min), after which the sample was washed with DI H_2O for 1 min and dried with a stream of N_2. The assembly bilayer was controlled to be two.

6. Preparation of $T(PE\text{-}M)_n$ (PE=PAH, PDDA, n=1) photoanodes

TNTAs substrate was firstly dipped into PAH (or PDDA) aqueous solution (0.5 mg/mL, 0.5 M NaCl, pH=10) for 1 min, washed with DI H_2O for 1 min and dried with a stream of N_2. Subsequently, PAH or PDDA-modified TNTAs was dipped into negatively charged MoS_2 QDs aqueous solution (25 mg/L) for 1 min, after which the sample was washed with DI H_2O for 1 min and dried with a stream of N_2.

7. Preparation of $T(B\text{-}PSS)_2$ photoanodes

TNTAs substrate was firstly dipped into BPEI aqueous solution (0.5 mg/mL, 0.5 M NaCl, pH=10) for 1 min, washed with DI H_2O for 1 min and dried with a stream of N_2. Subsequently, BPEI-modified TNTAs was dipped into PSS (0.5 mg/mL, 0.5 M NaCl, pH=10) aqueous solution for 1 min, after which the sample was washed with DI H_2O for 1 min and dried with a stream of N_2. The assembly bilayer was controlled to be two.

8. Preparation of Au nanoparticle-BPEI clusters[S1]

A solution of BPEI (25000 Da, 10 mg/mL in DMF) and a solution of $HAuCl_4$ (10 mg/mL in DMF) were prepared. 400 μL of each solution were added into 10 mL of DMF in a small glass vial and the mixture was immersed in an oil bath at 150 °C (corresponding to an internal temperature of ~130 °C (after 20 min) and stirred for 20 min at 700 rpm and finally cooled to room temperature.

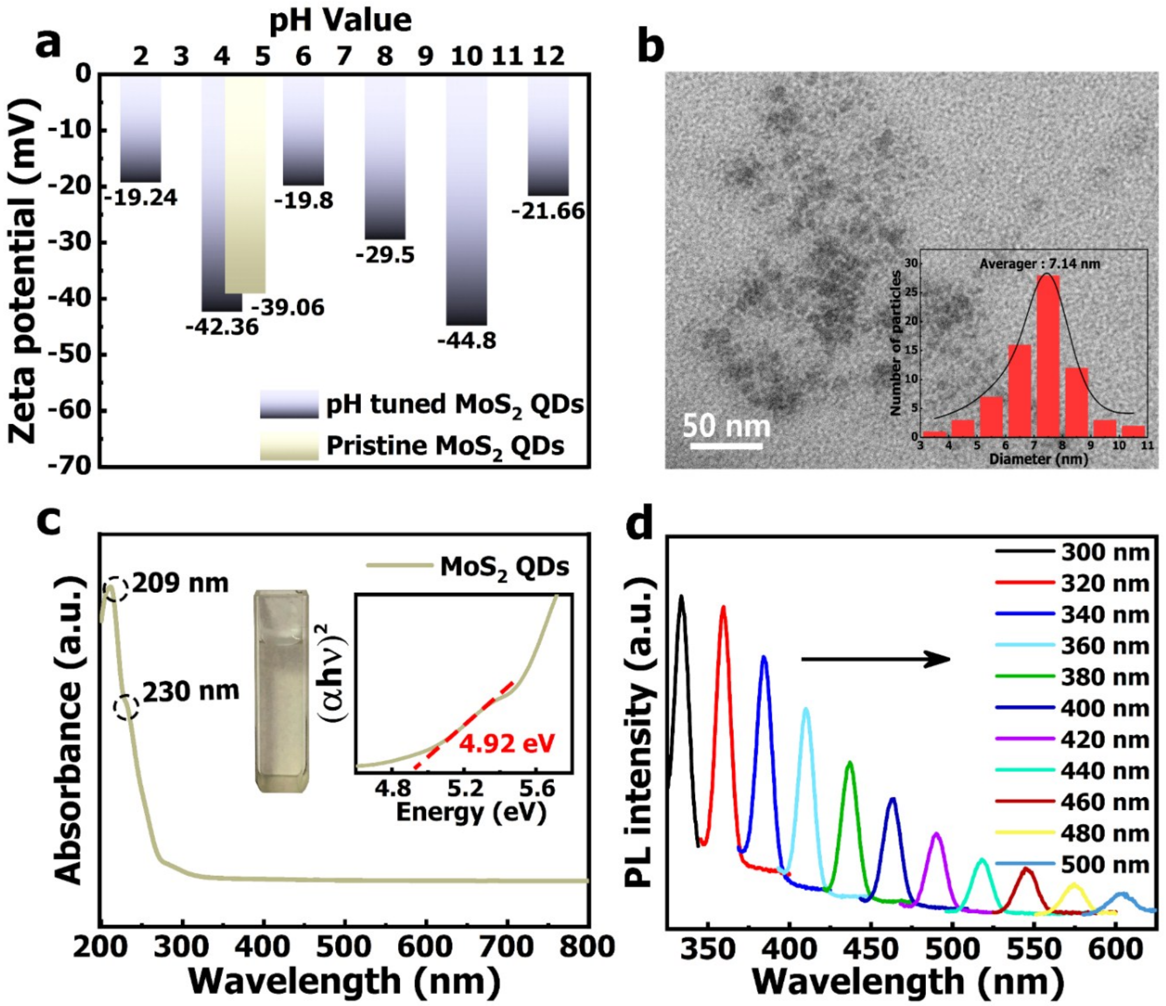

Fig. S1. (a) Zeta potentials and (b) TEM image with corresponding size distribution histogram in the inset, (c) UV-vis absorption spectrum with photograph and band-gap energy determination in the inset, and (d) PL spectra of MoS_2 QDs aqueous solution under different excitation wavelength.

Note: Two peaks at 209 and 230 nm were observed in the UV-vis absorption spectrum of MoS_2 QDs aqueous solution (**Fig. S1c**), which is attributed to the excitonic features of MoS_2 QDs.[S2] Band-gap energy of MoS_2 QDs is calculated to be 4.92 eV, larger than that of monolayer MoS_2 (1.9 eV) and bulk MoS_2 (1.2 eV), and similar to that of monolayered MoS_2 QDs (4.96 eV), attributable to the quantum size effect.[S3]

Fig. S1d shows the PL spectra of MoS_2 QDs aqueous solution excited by different wavelength (300~500 nm), wherein a red shift in the luminescence emission was observed with increasing the excitation wavelength (λ_{ex}), and its intensity decreases rapidly with increasing the emission wavelengths (450 to 600 nm). This suggests polydispersity of MoS_2 QDs, consistent with previous reports.[S4, 5]

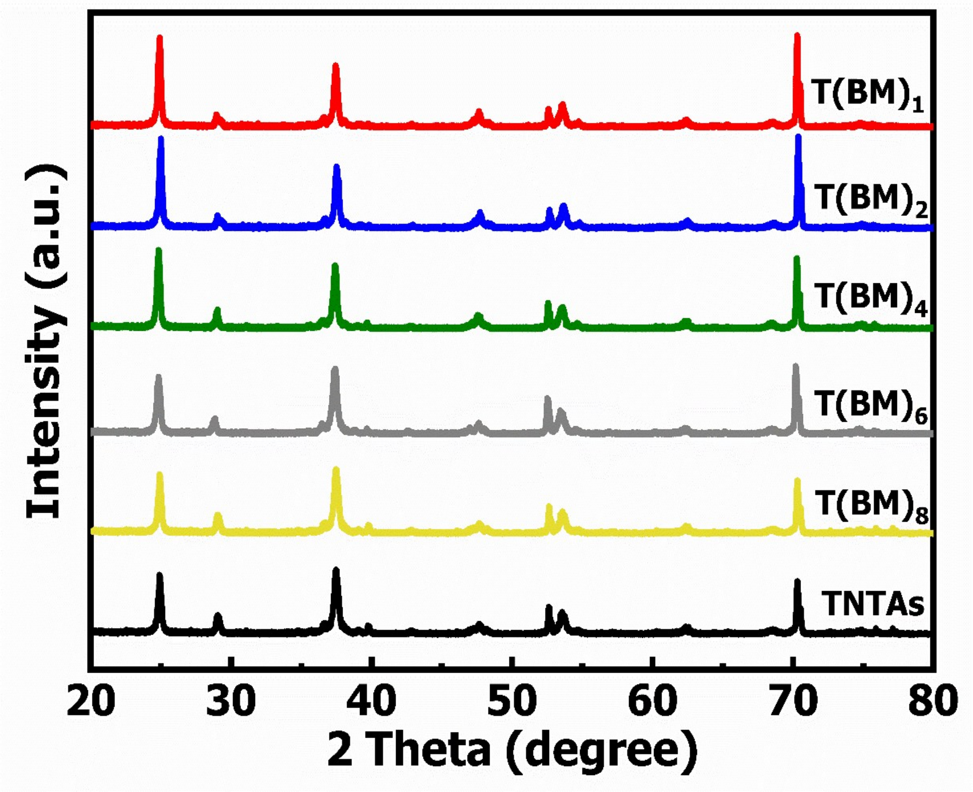

Fig. S2. XRD patterns of T(BM)$_n$ (n=1, 2, 4, 6, 8) multilayered photoanodes.

Table S1. Peak position with corresponding functional groups for $T(BM)_2$ and TNTAs.

Peak position (cm^{-1})	***$T(BM)_2$***	***TNTAs***
3430	N-H and O-H stretching vibration	O-H stretching vibration
2920	C-H stretching vibration	N.D.
2860	C-H stretching vibration	N.D.
1630	N-H and O-H deformation vibration	O-H deformation vibration
1390	Ti-O stretching vibrations	Ti-O stretching vibrations
1110	C-N stretching vibrations	N.D.
823	Ti-O stretching vibrations	Ti-O stretching vibrations

N.D.: Not Detected.

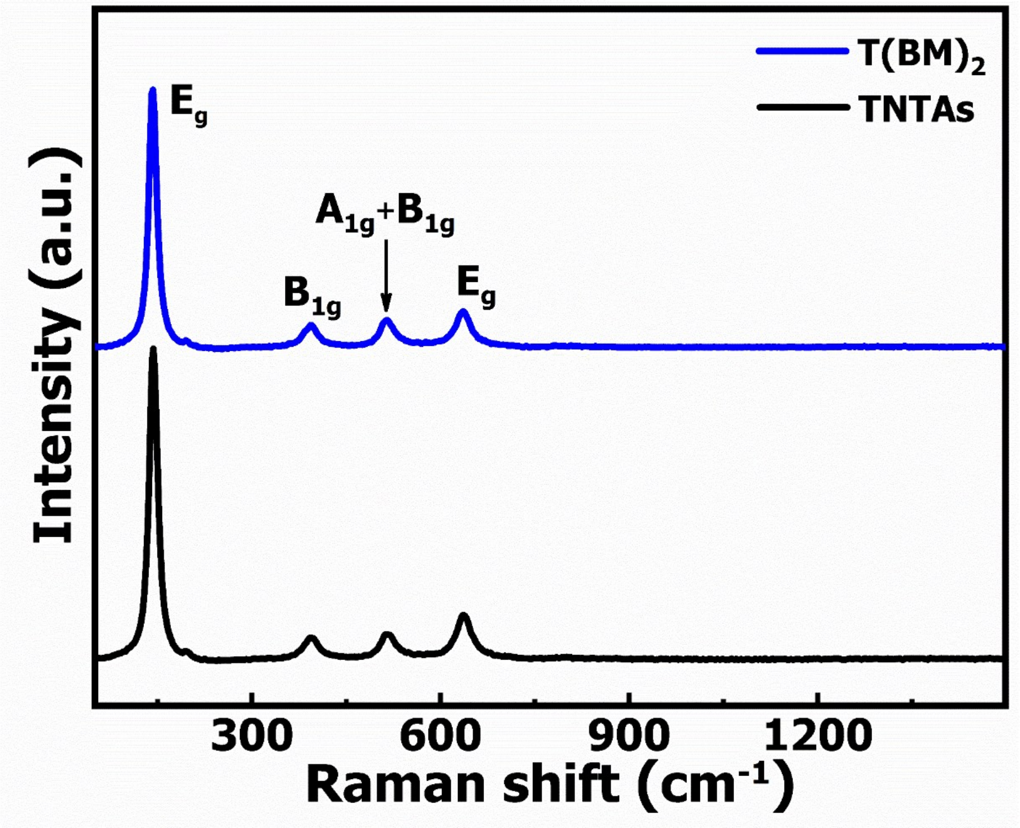

Fig. S3. Raman spectra of T(BM)$_2$ and TNTAs.

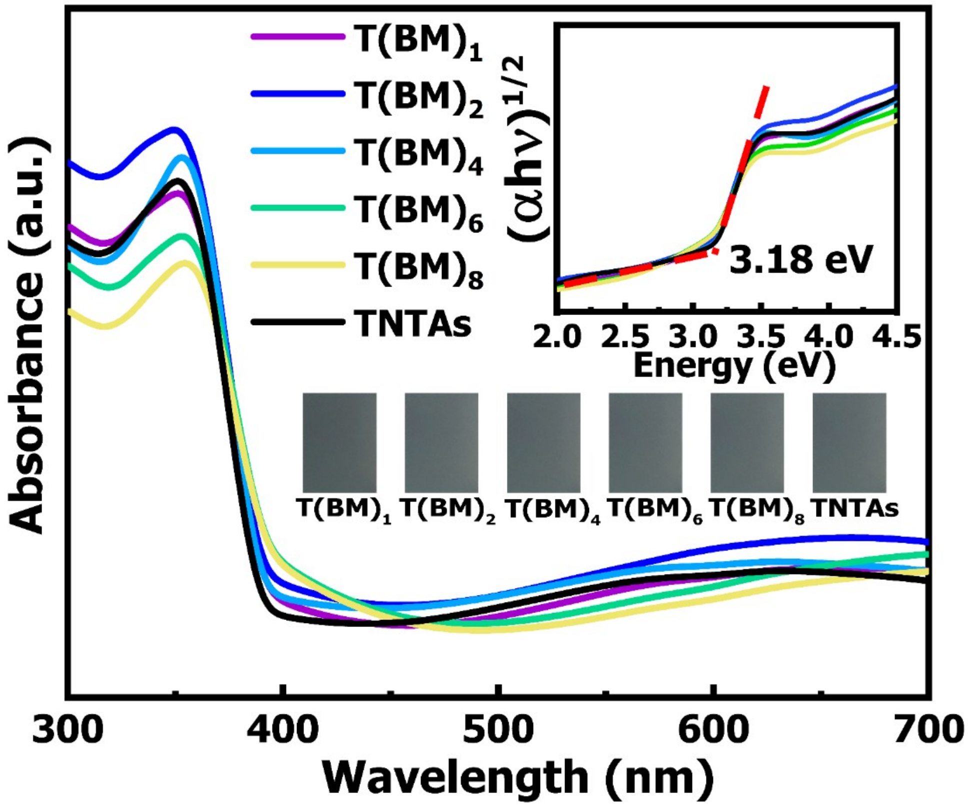

Fig. S4. DRS results of T(BM)$_n$ (n=1, 2, 4, 8) and TNTAs with corresponding photographs and bandgap determination in the inset.

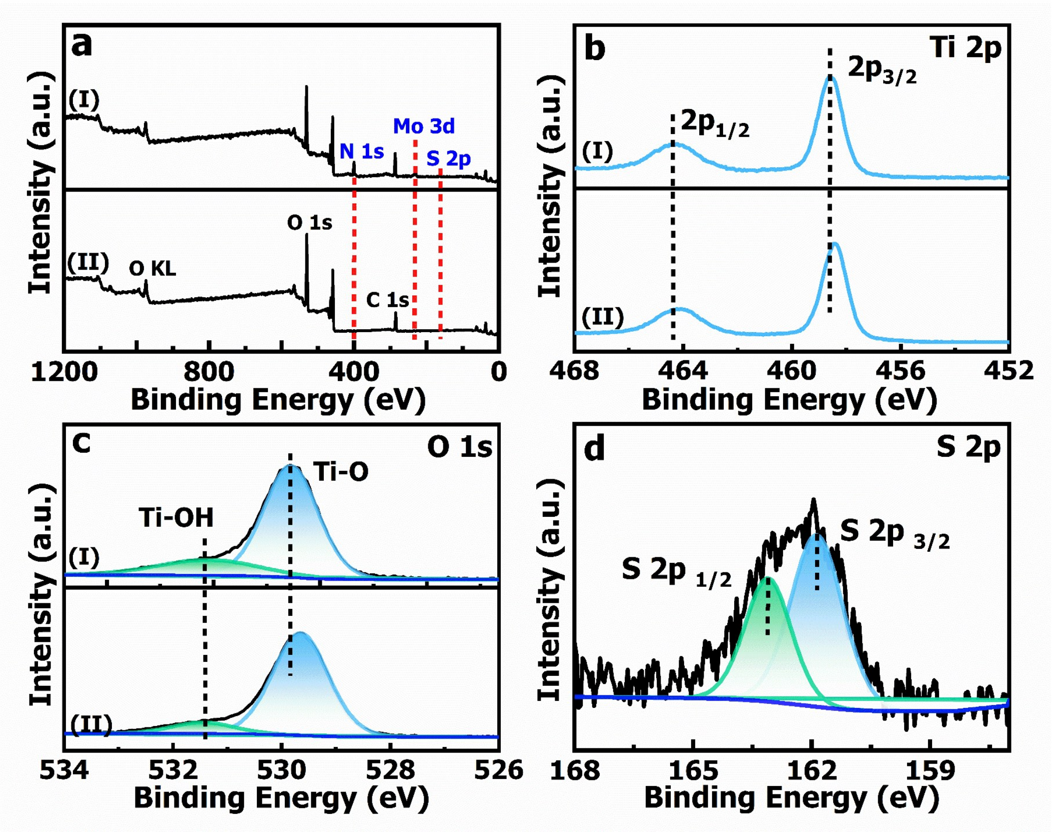

Fig. S5. (a) Survey spectra of (I) $T(BM)_2$ and (II) TNTAs, high-resolution (b) Ti 2p and (c) O 1s spectra of (Ⅰ) $T(BM)_2$ and (Ⅱ) TNTAs, and high-resolution (d) S 2p spectrum of $T(BM)_2$.

Table S2. Chemical bond species vs. B.E. for different photoelectrodes.

Element	*$T(BM)_2$*	*TNTAs*	*Chemical Bond Species*
Ti $2p_{3/2}$	458.70	458.40	Anatase (4+)
Ti $2p_{1/2}$	464.45	464.10	Anatase (4+)[S6]
O 1s A	529.95	529.65	Lattice Oxygen
O 1s B	531.60	531.45	Ti-OH[S7]
N 1s A	398.50	N.D.	$-NH-/-NH_2-$
N 1s B	399.60	N.D.	C-N
N 1s C	400.20	N.D.	$-NH_3^+$
Mo $3d_{5/2}$	228.87	N.D.	Mo^{3+}
Mo $3d_{3/2}$	232.40	N.D.	Mo^{3+}
S $2p_{3/2}$	161.88	N.D.	S^{2-}
S $2p_{1/2}$	163.10	N.D.	S^{2-}

N.D.: Not Detected.

Note: Some typical chemical bond species, such as carboxylate, lattice oxygen, and Ti-OH in $T(BM)_2$ show concurrent substantial shifts in B.E., thus once again indicating the pronounced interaction among ultra-thin BPEI layer, MoS_2 QDs and TNTAs substrate.

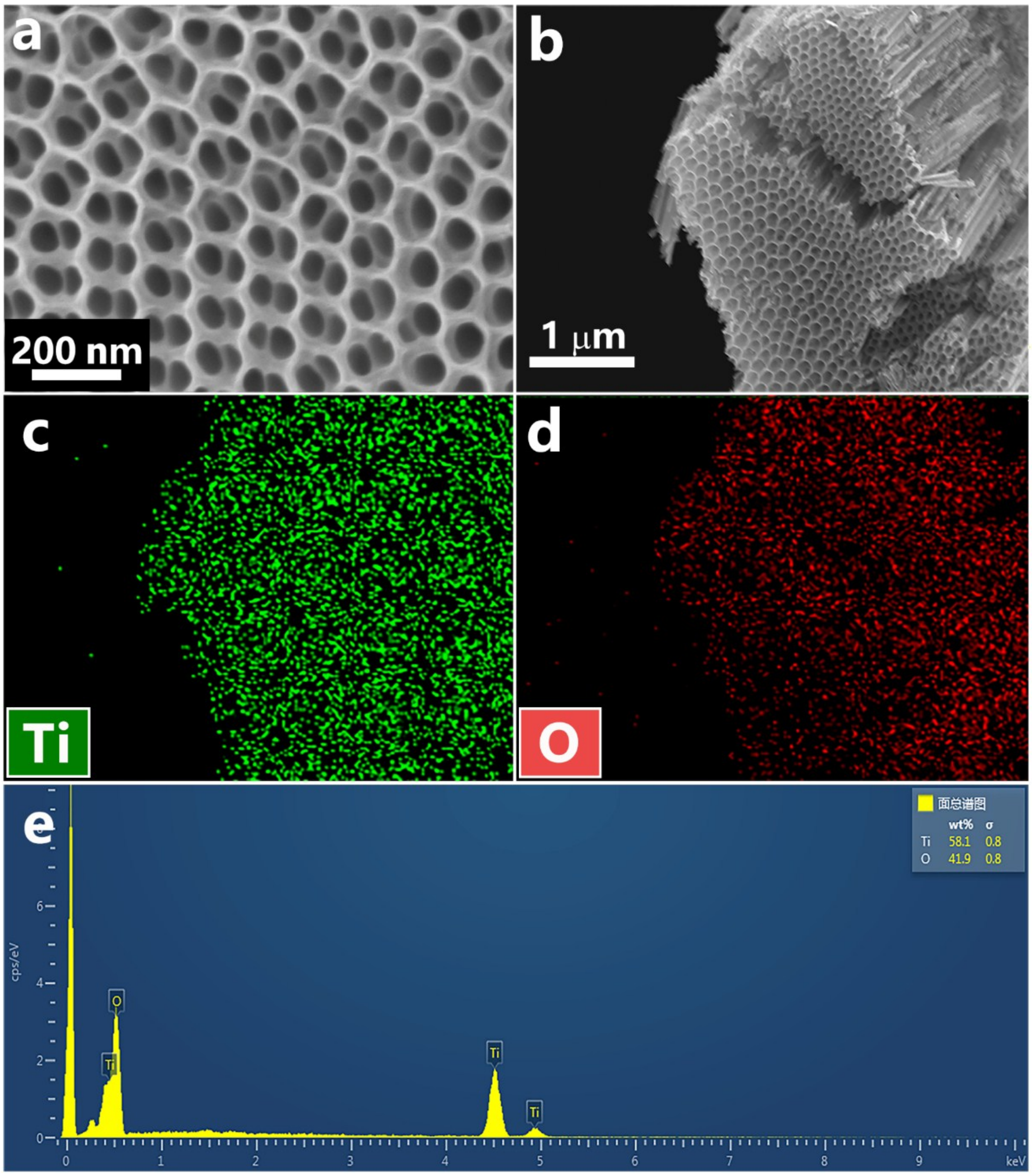

	wt%	σ
Ti	58.1	0.8
O	41.9	0.8

Fig. S6. (a & b) FESEM images of TNTAs with corresponding (c & d) elemental mapping and (e) EDS results.

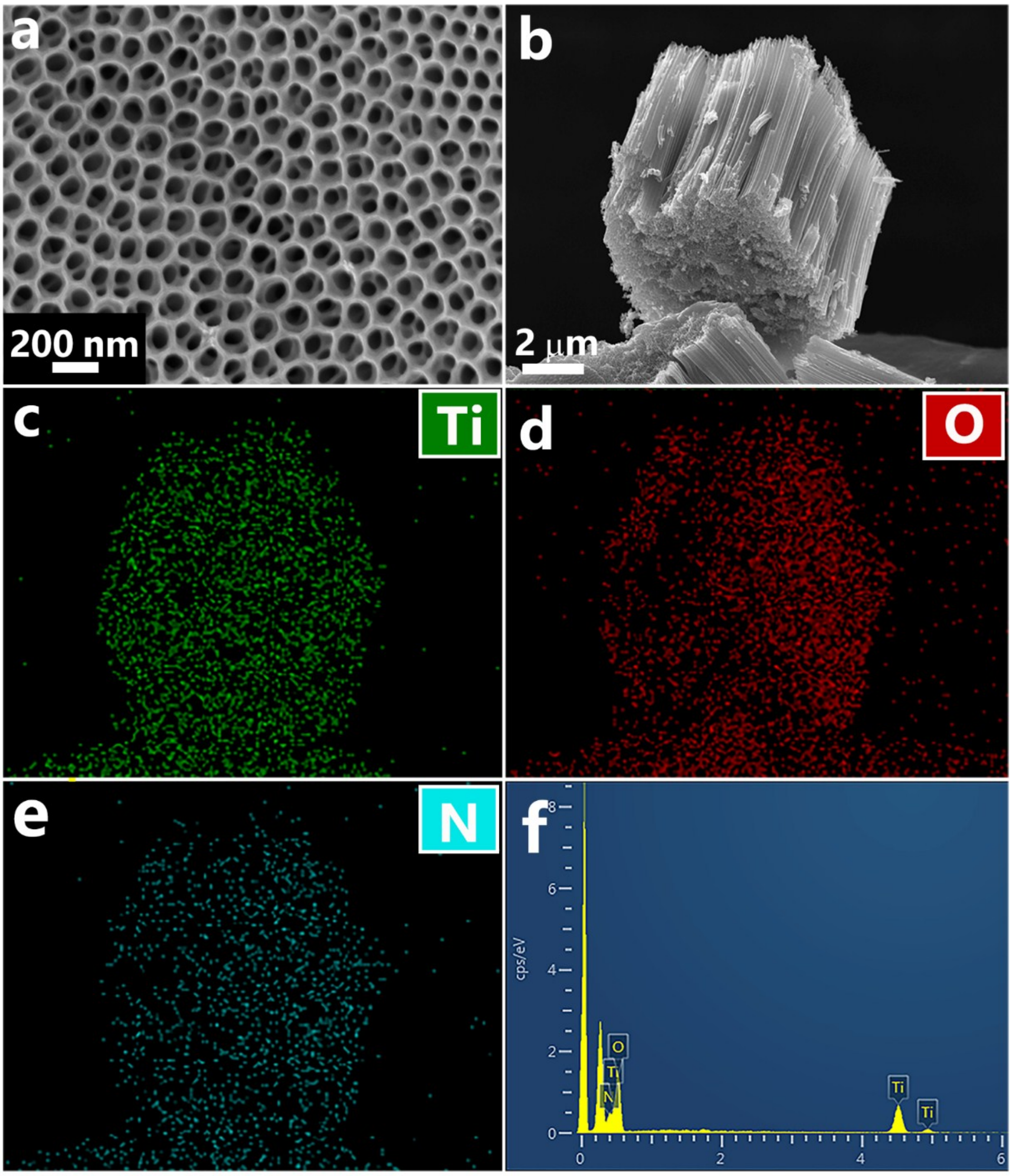

Fig. S7. (a) Top-view and cross-section FESEM images of TB_2 with corresponding (b-e) elemental mapping and (f) EDS results.

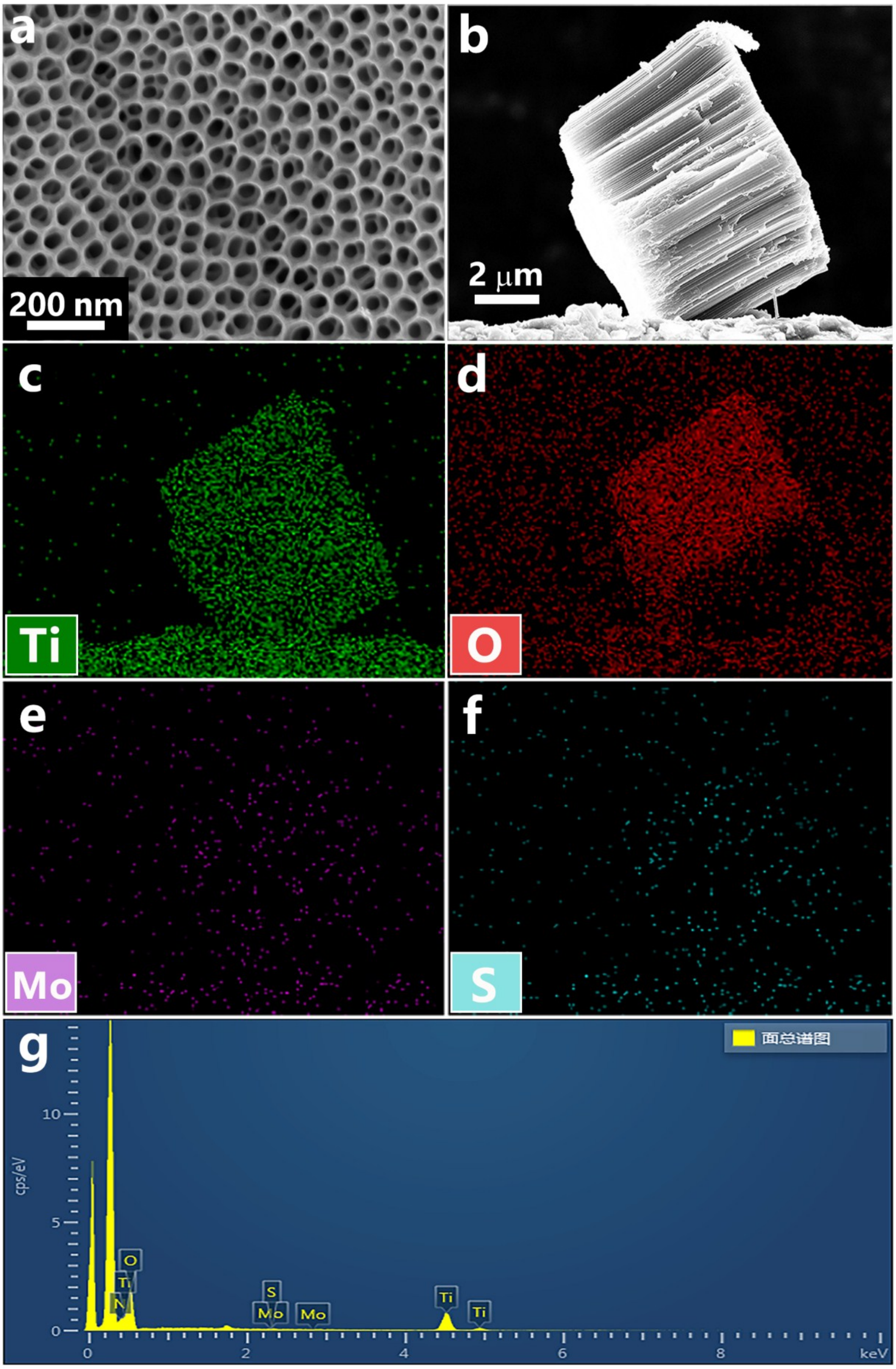

Fig. S8. (a) Top-view and cross-section FESEM images of TM_2 with corresponding (b-f) elemental mapping and (g) EDS results.

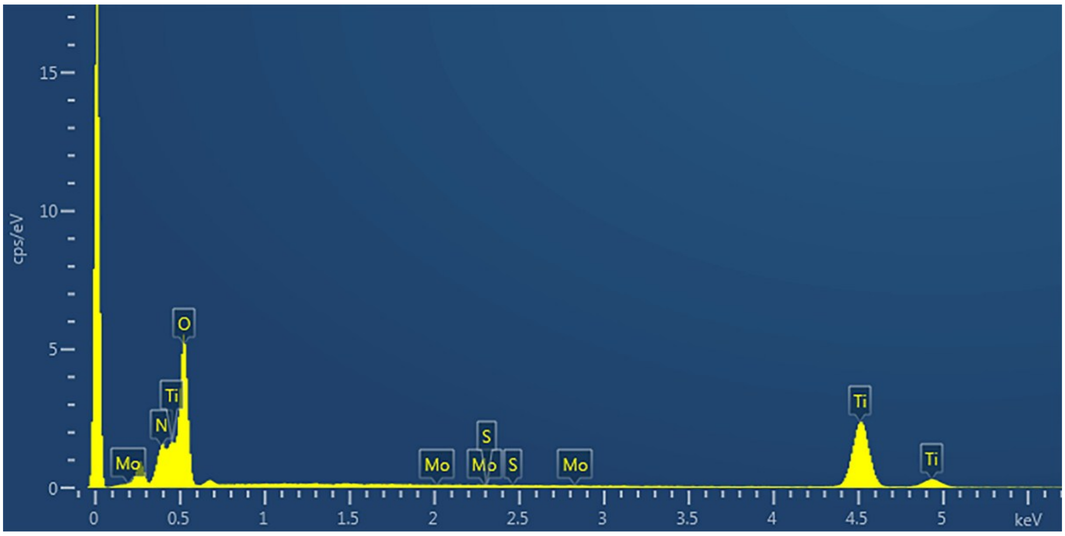

Fig. S9. EDS result of $T(BM)_2$ heterostructure.

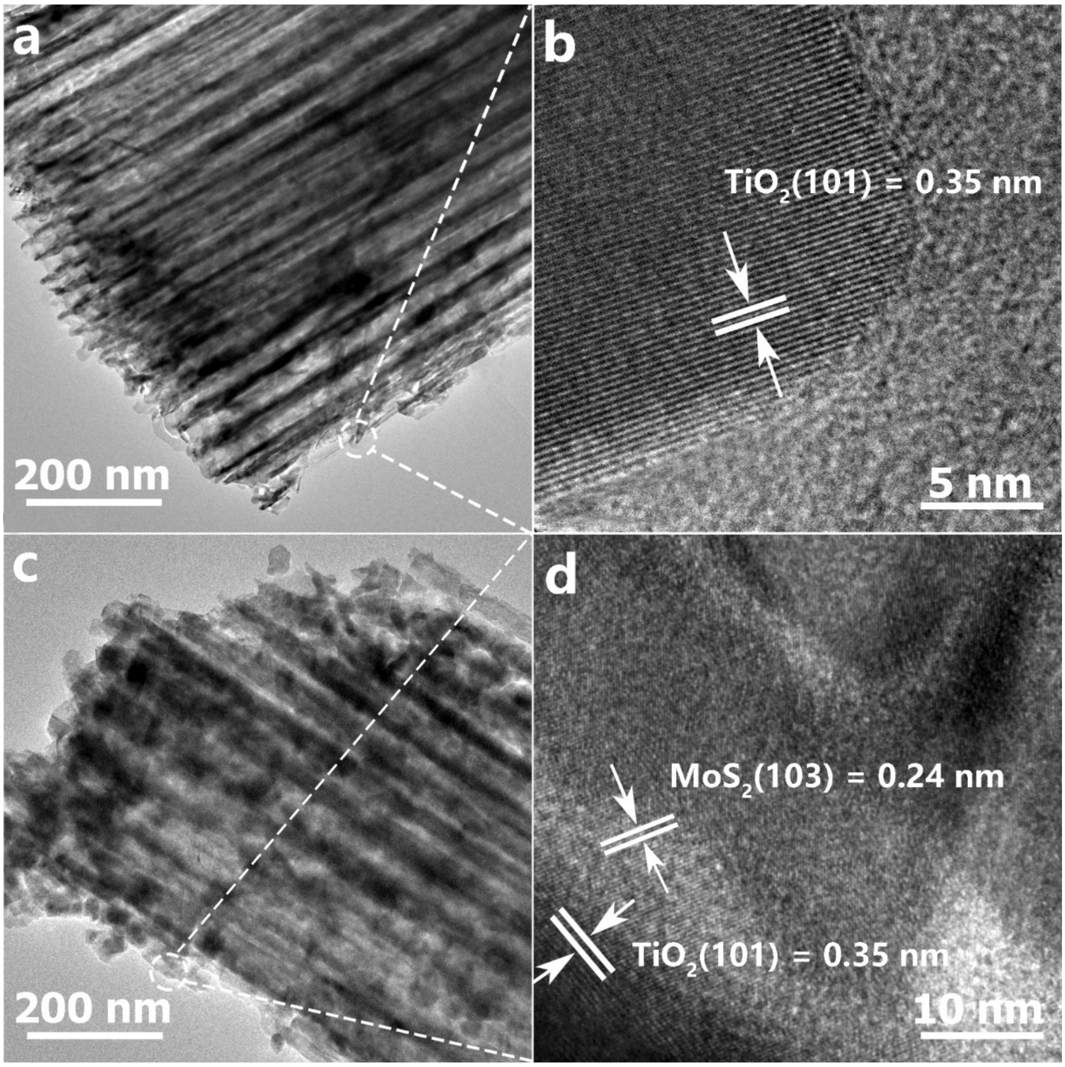

Fig. S10. (a & c) TEM and (b& d) HRTEM images of (a & b) TNTAs and (c & d) T(BM)$_2$.

Note: Successful deposition of MoS$_2$ QDs on the T(BM)$_2$ can also be verified by **Fig. S6d** which exhibits the typical (103) crystal plane of MoS$_2$ QDs with distinct lattice fringe of 0.24 nm.

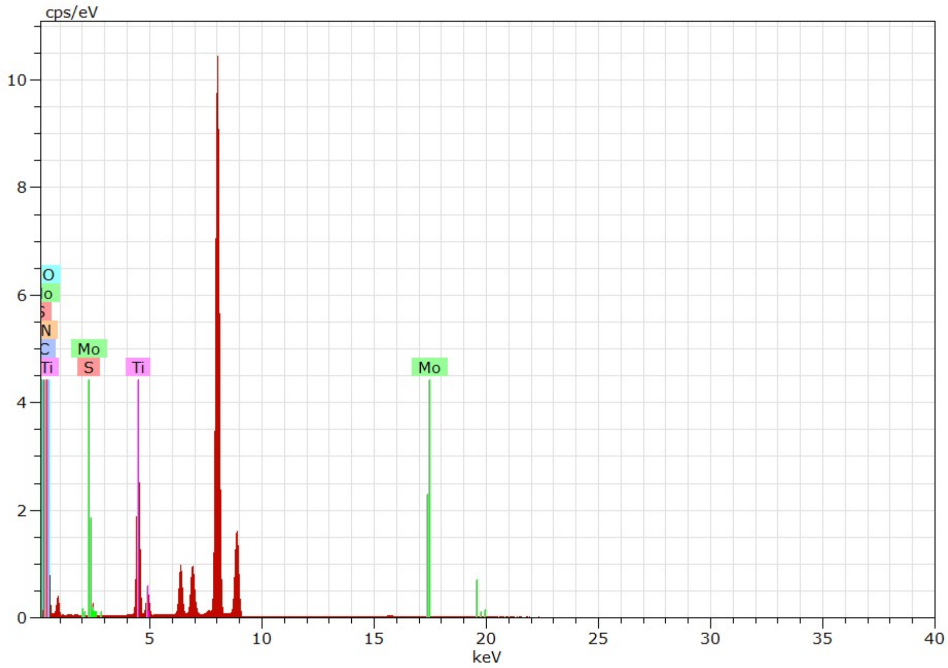

Fig. S11. TEM EDS result of $T(BM)_2$ heterostructure.

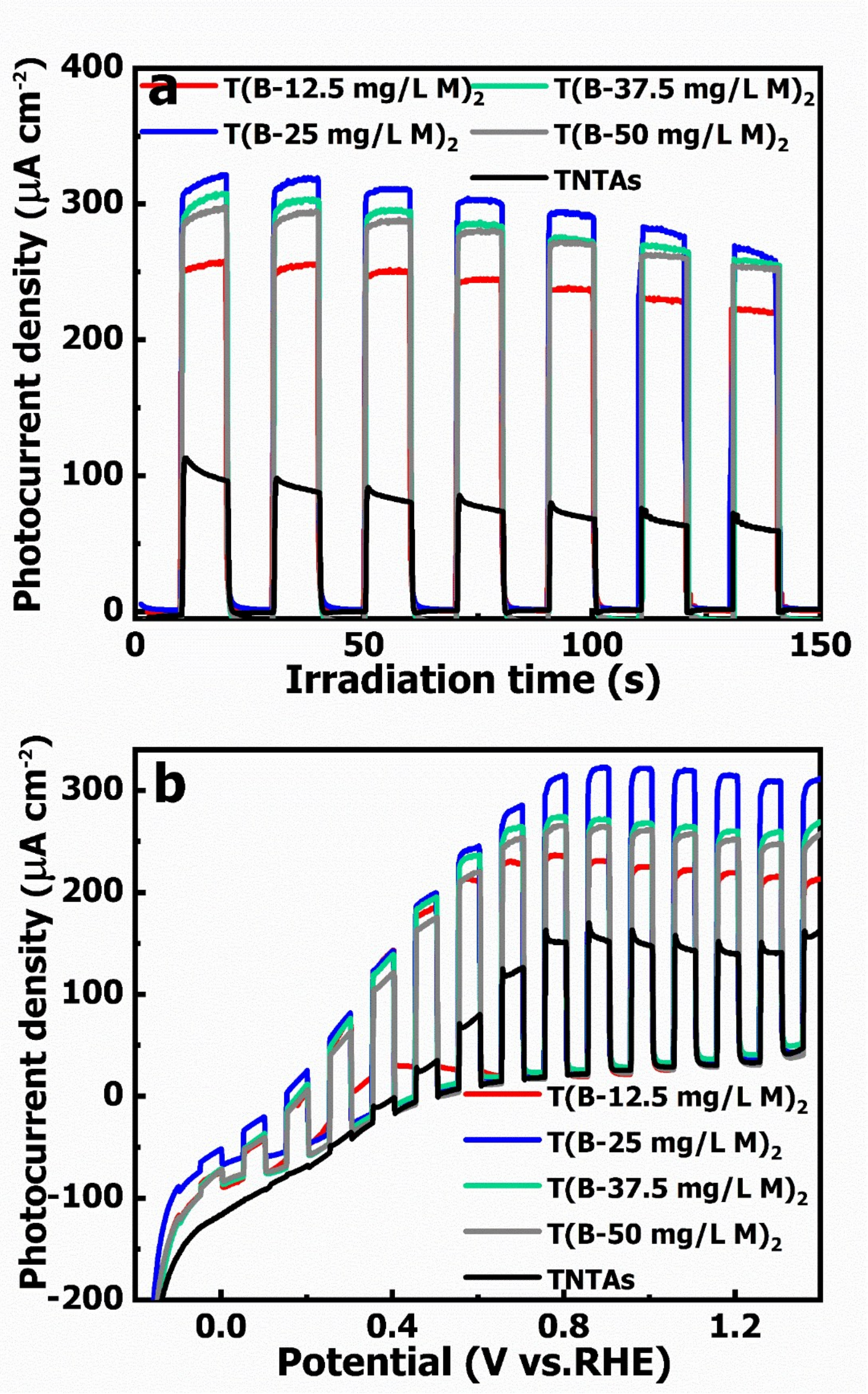

Fig. S12. (a) On-off transient photocurrent and (b) LSV results of T(B-XM)$_2$ (X=12.5, 25, 37.5, 50 mg/L) prepared by utilizing different concentration of MoS_2 QDs under simulated solar light irradiation (AM1.5G).

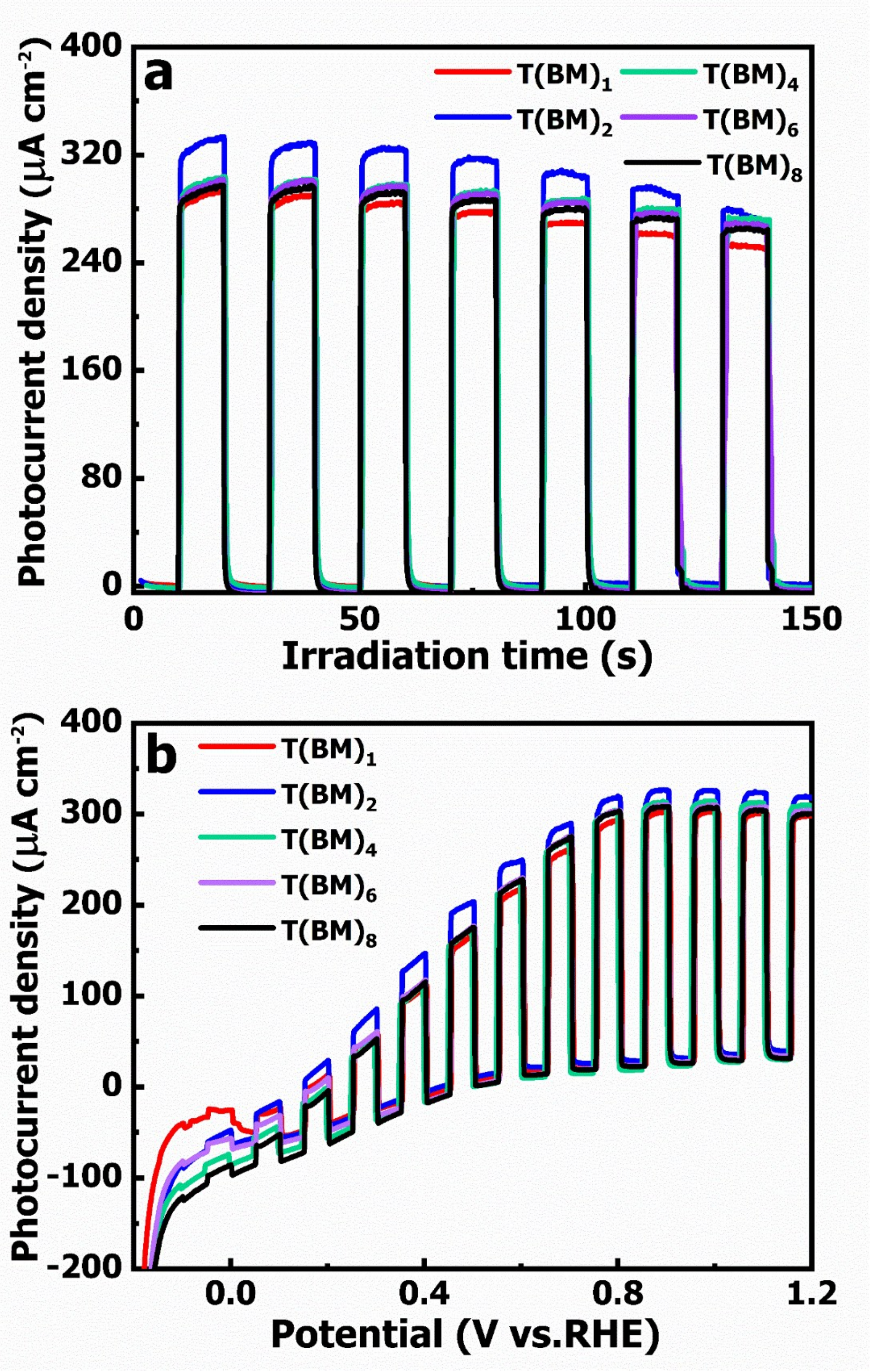

Fig. S13. (a) On-off transient photocurrent and (b) LSV results of T(BM)$_n$ (n=1, 2, 4, 6, 8) multilayered heterostructures under solar light irradiation (AM1.5G).

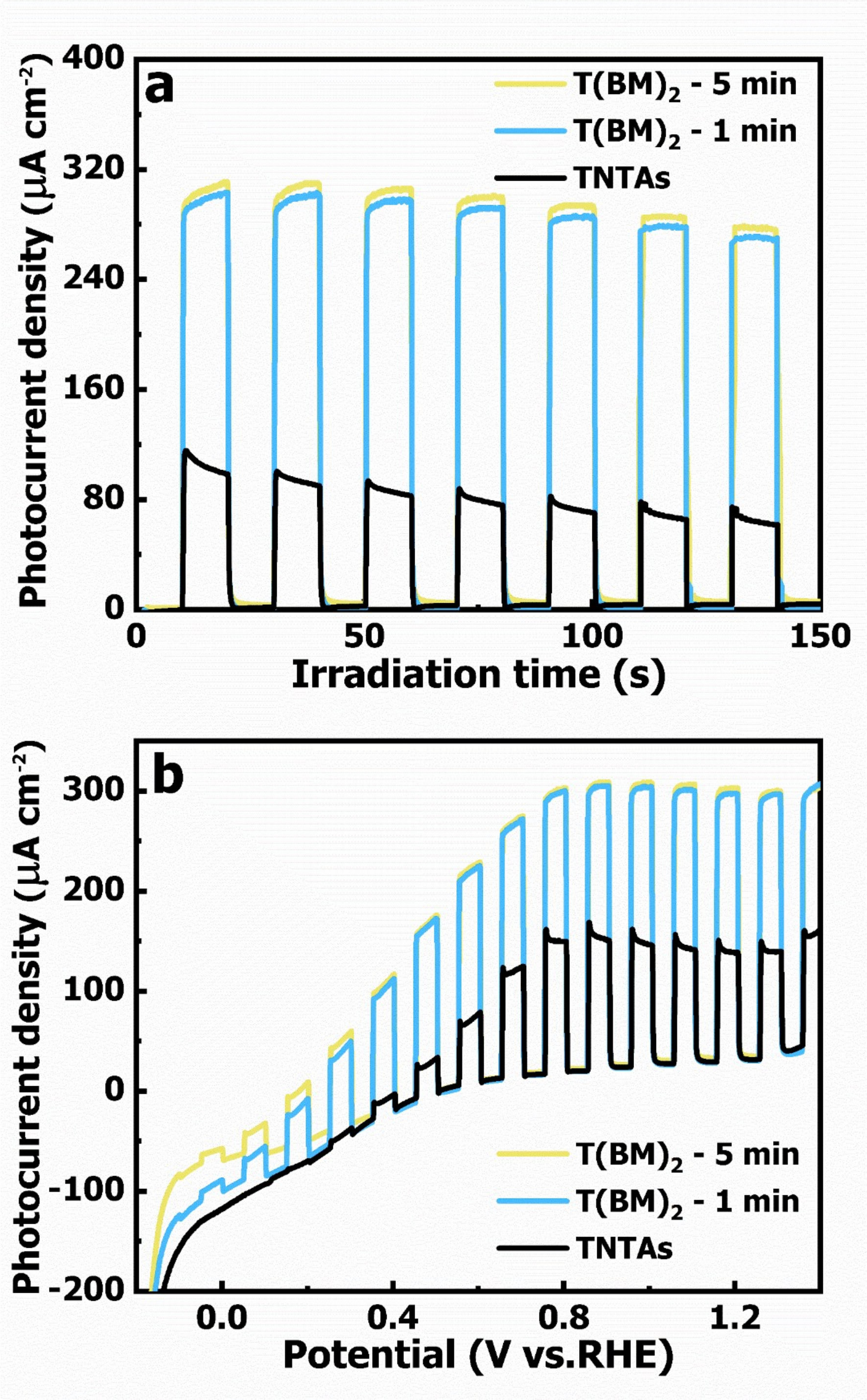

Fig. S14. (a) On-off transient photocurrent and (b) LSV results of $T(BM)_2$ with different deposition time for each assembly bilayer under simulated solar light irradiation (AM1.5G).

Note: The different deposition time at each LbL assembly bilayer means that TNTAs substrate was first dipped into positively charged BPEI aqueous solution for 1 min (or 5 min) and then washed with DI H_2O for 1 min. Subsequently, BPEI-modified TNTAs was dipped into negatively charged MoS_2 QDs aqueous solution for 1 min (or 5 min), after which the sample was washed with DI H_2O for 1 min.

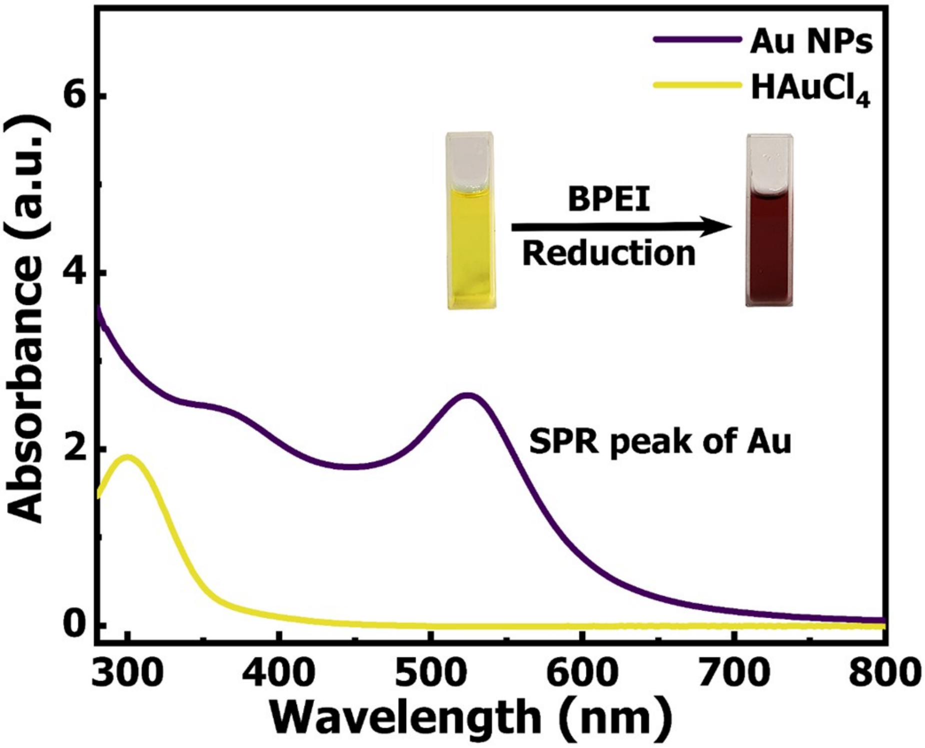

Fig. S15. UV-vis absorption spectra of $HAuCl_4$ solution before and after adding BPEI.

Note: Color of tetrachloroauric acid solution changes from paint yellow to wine after adding the BPEI, indicating $HAuCl_4$ precursor has been completely reduced to Au nanoparticles and this can also be corroborated by the UV-vis absorption spectrum of the $HAuCl_4$/BPEI mixed solution with the presence of a characteristic SPR peak of Au NPs. The results strongly evidence the intrinsic strong reducing capability of BPEI.[S1] That is, BPEI is able to mediate the hole transfer.

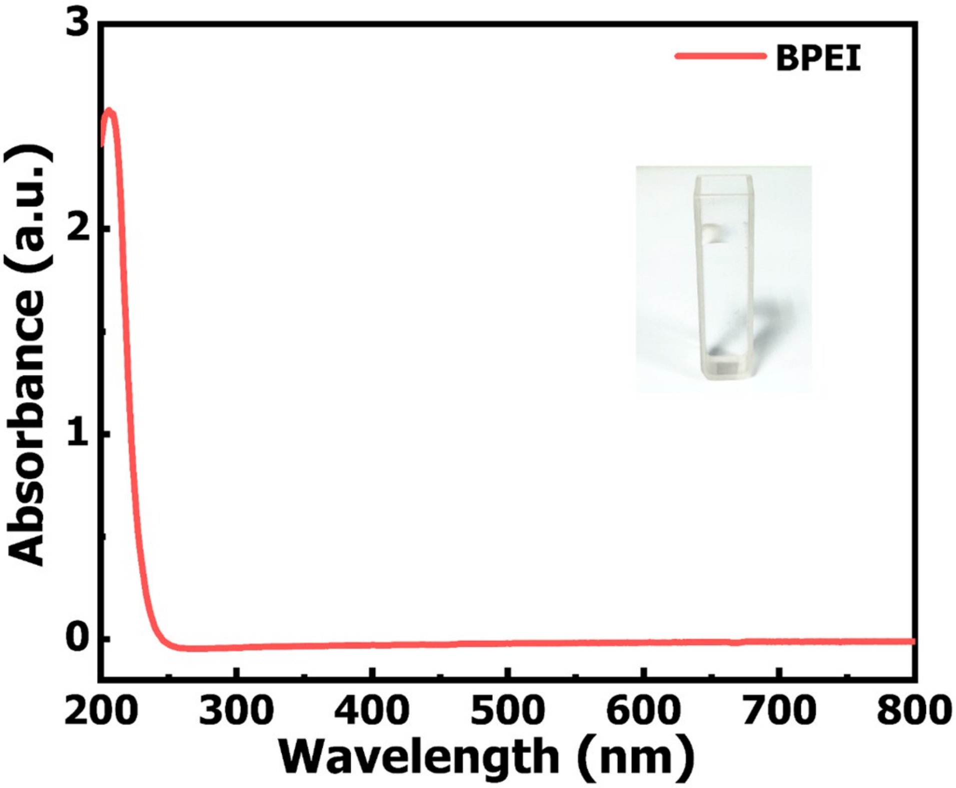

Fig. S16. UV-vis absorption spectrum of BPEI aqueous solution.

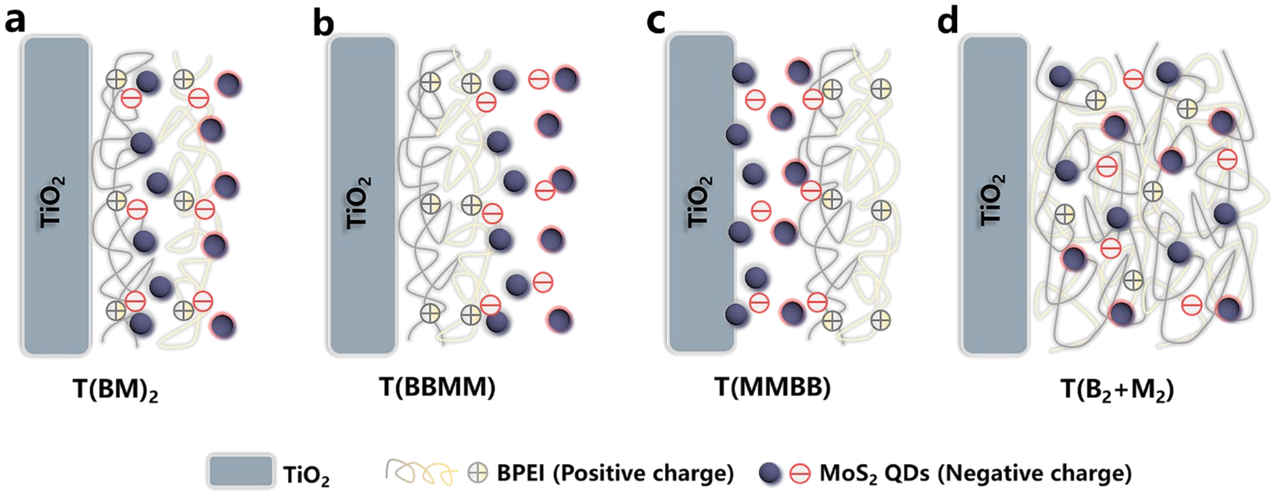

Fig. S17. Schematic illustration of TNTAs/BPEI/MoS_2 QDs ternary photoanodes with different stacking fashion.

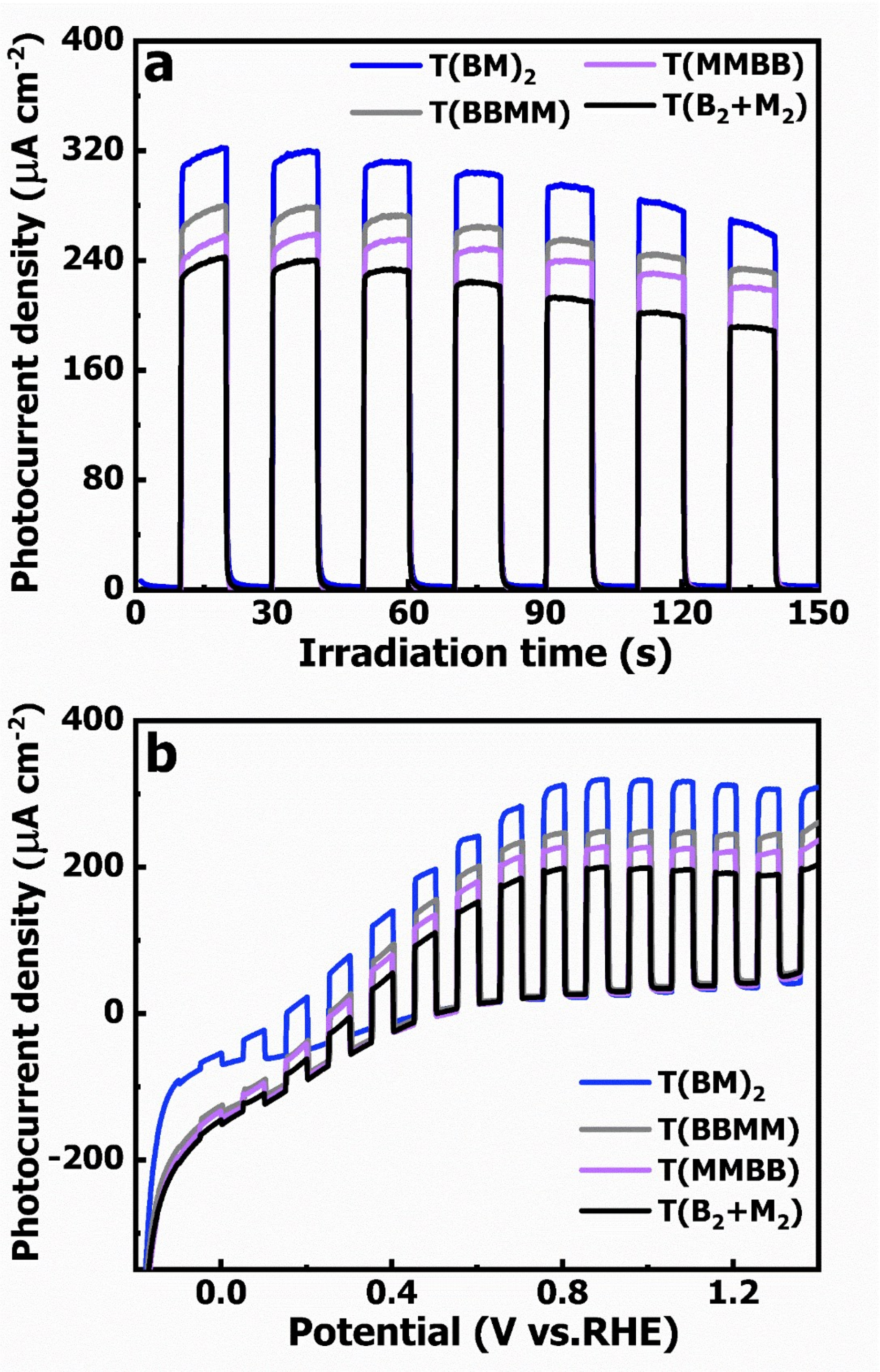

Fig. S18. (a) On-off transient photocurrent and (b) LSV results of T(BM)$_2$ with different stacking fashion under simulated solar light irradiation (AM1.5G).

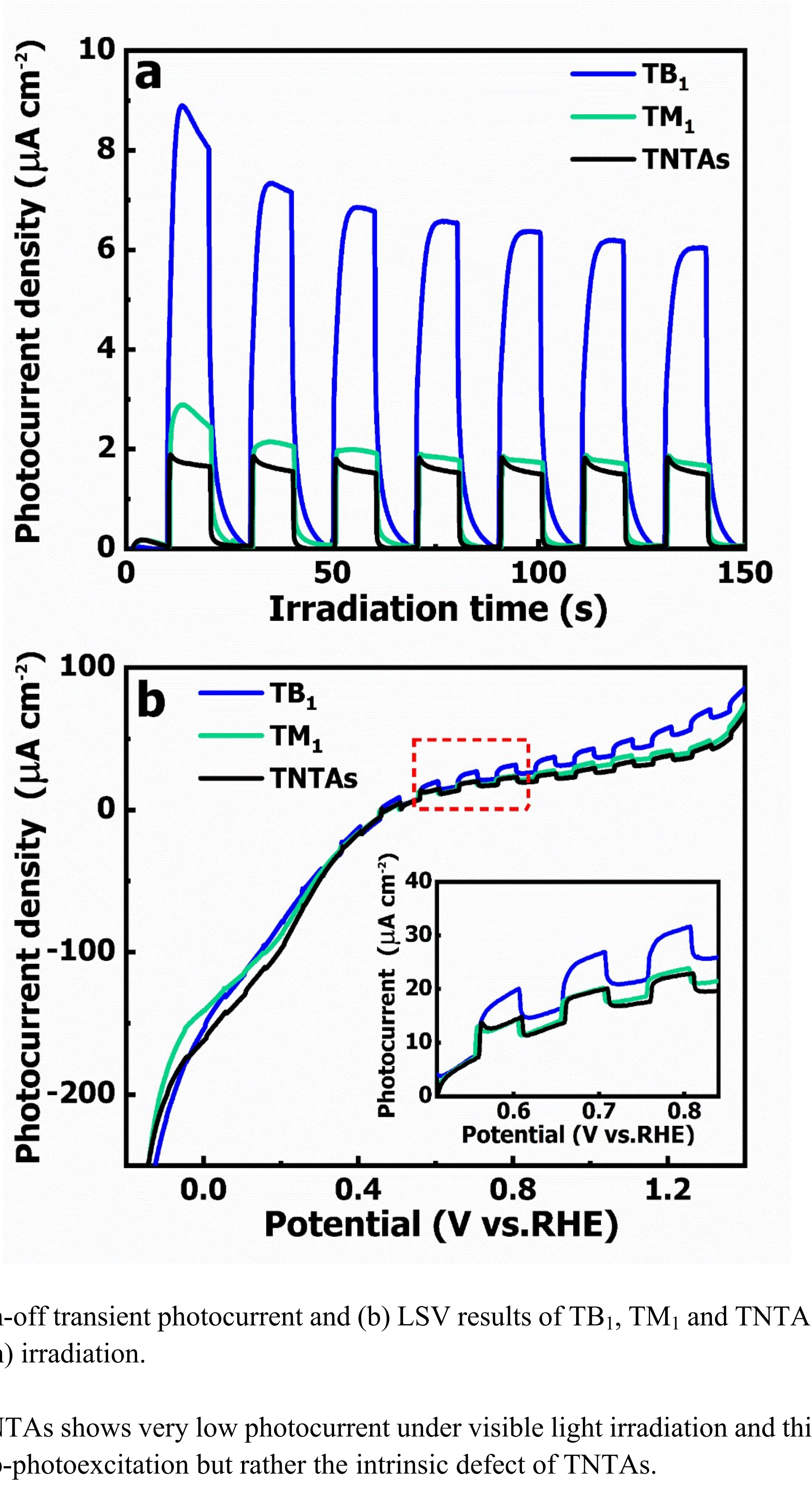

Fig. S19. (a) On-off transient photocurrent and (b) LSV results of TB$_1$, TM$_1$ and TNTAs under visible light (λ>420 nm) irradiation.

Note: Blank TNTAs shows very low photocurrent under visible light irradiation and this is not caused by the band-gap-photoexcitation but rather the intrinsic defect of TNTAs.

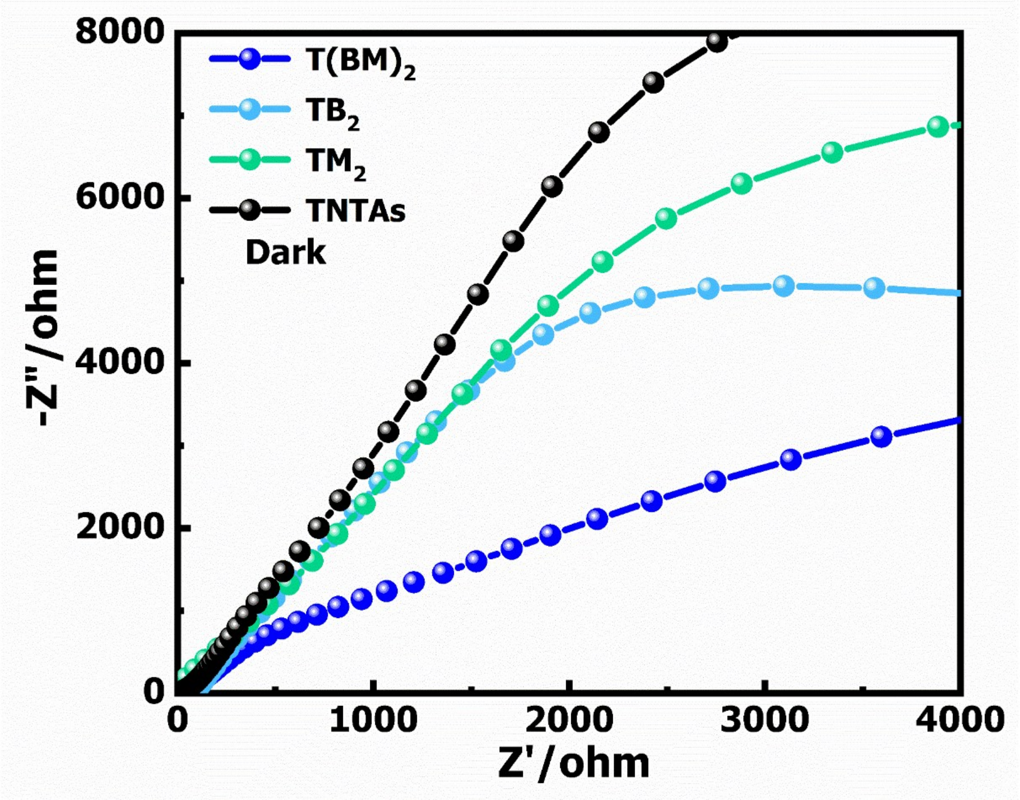

Fig. S20. EIS results of different photoanodes in dark.

Table S3. Fitted EIS results of different photoanodes under simulated solar light irradiation based on the equivalent circuit.

Photoanodes	R_s/ohm	R_{ct}/ohm	CPE /(F·cm^{-2})
T(BM)$_2$	6.337	786	2.443E-5
TB$_2$	33.52	1211	0.0004959
TM$_2$	50.33	2963	0.0004082
TNTAs	59.88	3037	0.0004022
Ti(BM)$_2$	5.827	21560	3.1595E-5

Note: As shown in **Table S3**, R_{ct} values were obtained by fitting the EIS results according to a simple equivalent circuit composed of a series of resistance (**Fig. 4d**, inset). Apparently, T(BM)$_2$ demonstrated the smallest R_{ct} value in comparison with other counterparts, indicative of the lowest charge transfer resistance in the interfacial region.

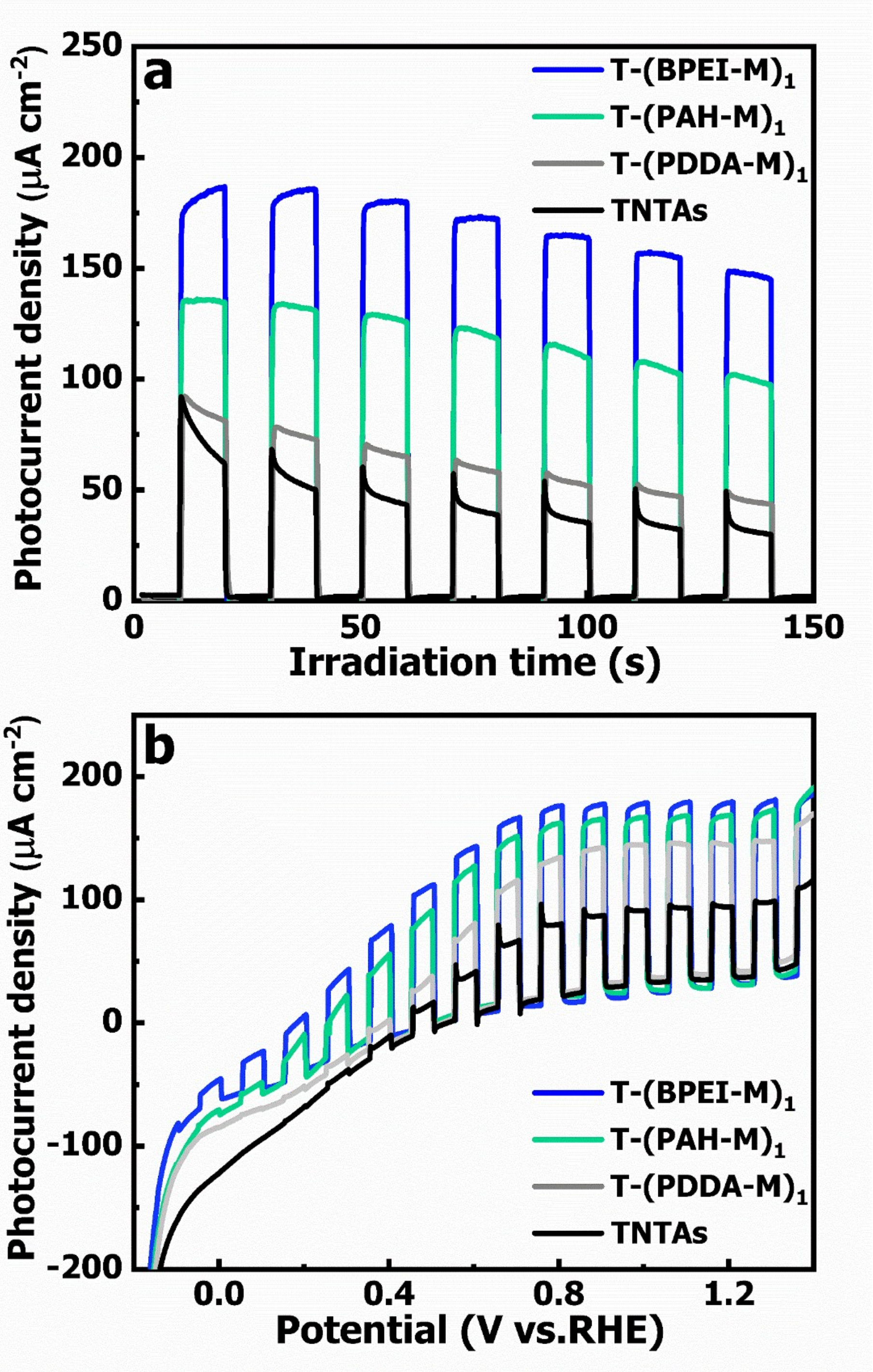

Fig. S21. (a) & (b) On-off transient photocurrent and LSV results (scan rate: 5 mV s^{-1}, bias voltage: 0.61 V vs. RHE) of T(PE-M)$_n$ (PE=BPEI, PAH, PDDA; n=1) in Na_2SO_4 aqueous solution (pH=6.69) under simulated solar light irradiation (AM1.5).

Table S4. Molecular structures of different polyelectrolytes.

Polyelectrolyte	*Chemical structure*	*Charge*
Polyethylenimine, Branched (BPEI)	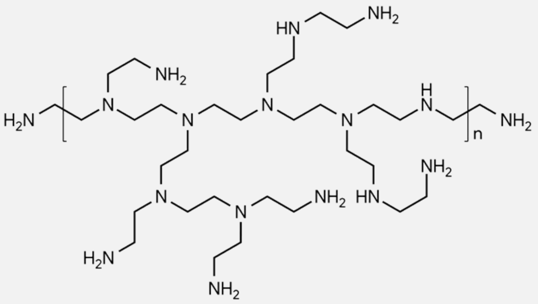	Positive charge
Poly (diallyldimethylammonium chloride) solution (PDDA)	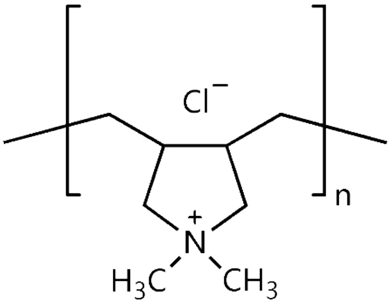	Positive charge
Poly (allyamine hydrochloride) (PAH)	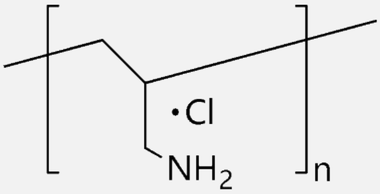	Positive charge
Poly (sodium 4-styrenesulfonate) solution (PSS)	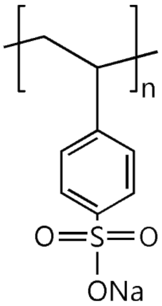	Negative charge

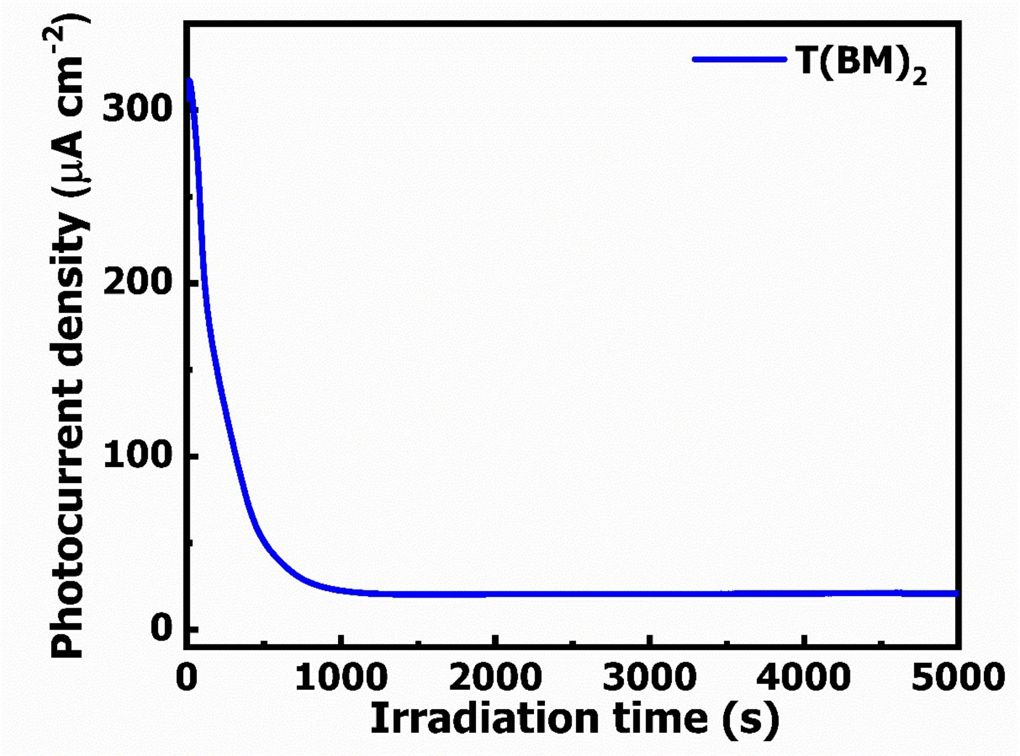

Fig. S22. Photocurrent of T(BM)$_2$ under continuous simulated solar light (AM1.5) irradiation in Na_2SO_4 aqueous solution (pH=6.69). (bias voltage: 0.61 V vs. RHE)

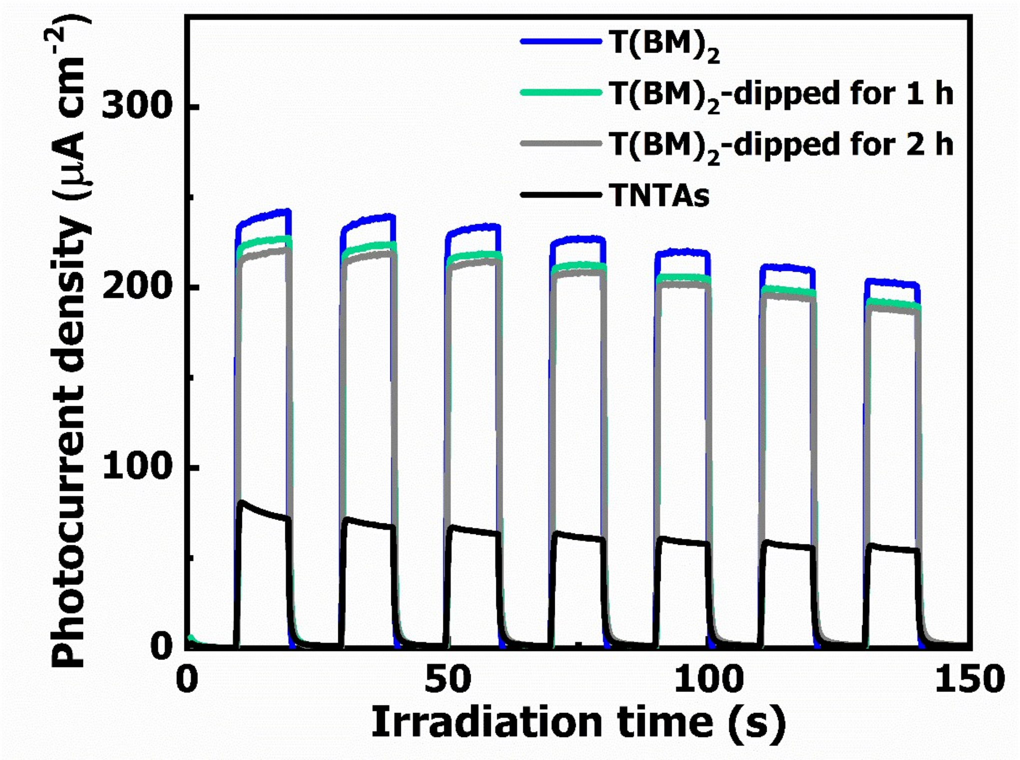

Fig. S23. On-off transient photocurrent of T(BM)$_2$ and T(BM)$_2$ after dipping in DI H_2O for 1 h and 2 h in Na_2SO_4 aqueous solution (pH=6.69) under simulated solar light irradiation (AM1.5).

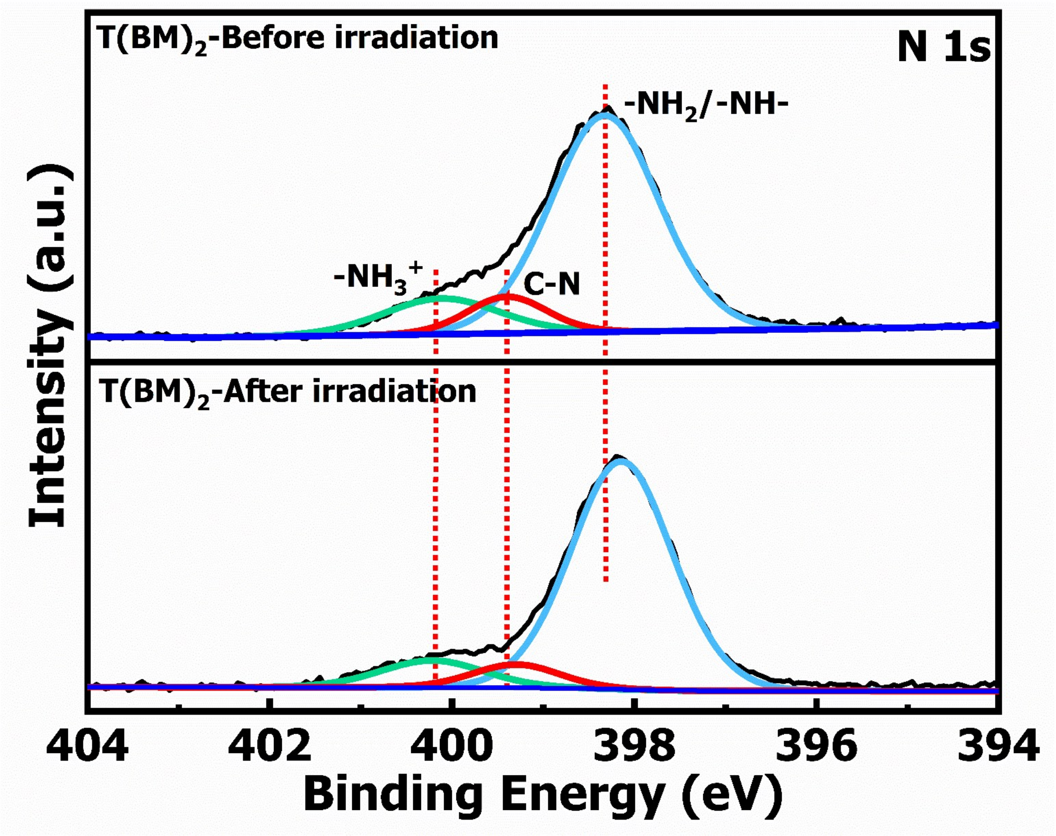

Fig. S24. High-resolution N 1s spectra of T(BM)$_2$ before and after consecutive simulated solar irradiation for 2 h.

Note: N element in the high-resolution N 1s spectrum of T(BM)$_2$ after consecutive simulated solar irradiation for 2 h shows no apparent B.E. shifts, i.e., ca. 0.16 eV for -NH/-NH$_2$ (i.e. 398.34 eV vs. 398.5 eV), 0.1 eV for N-C (i.e. 399.50 eV vs. 399.6 eV) and 0.02 eV for -NH$_3^+$ (i.e. 400.22 eV vs. 400.20 eV) as compared to freshly prepared T(BM)$_2$.

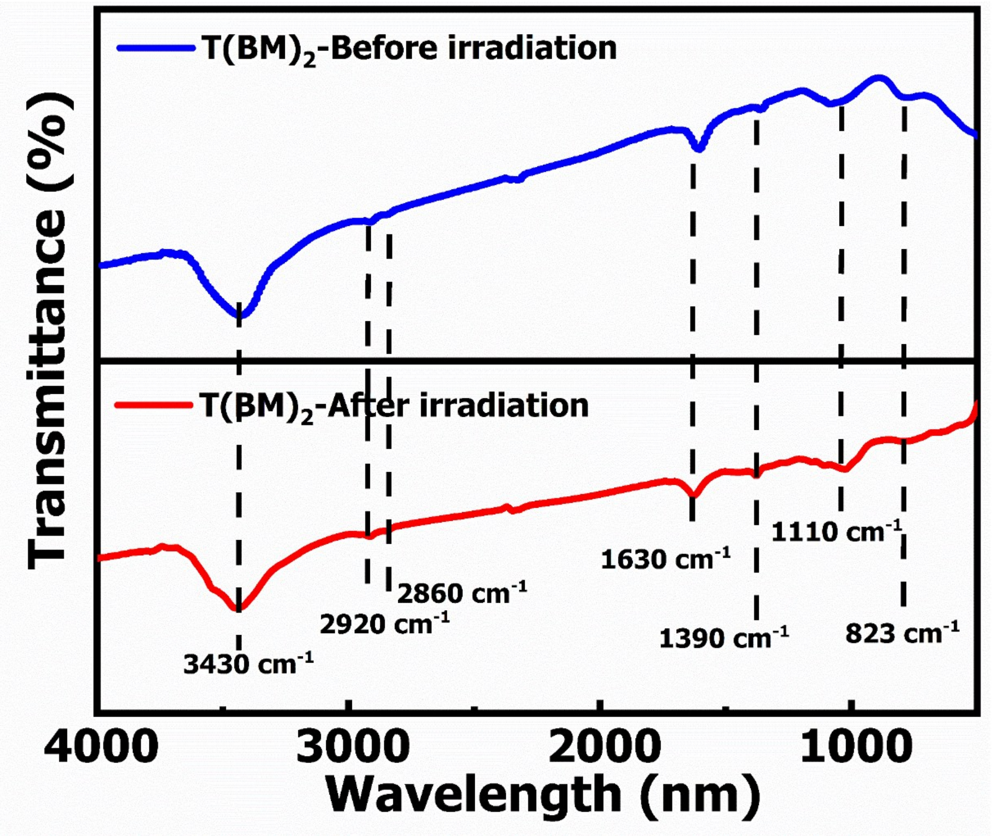

Fig. S25. FTIR spectra of T(BM)$_2$ before and after consecutive simulated solar irradiation for 2 h.

References

S1. F. Kretschmer, U. Mansfeld, S. Hoeppener, M. D. Hager and U. S. Schubert, *Chem Commun (Camb)*, 2014, **50**, 88-90.

S2. V. Chikan and D. F. Kelley, *J. Phys. Chem. B*, 2002, **106**, 3794-3804.

S3. H. Huang, C. Du, H. Shi, X. Feng, J. Li, Y. Tan and W. Song, *Part. Part. Syst. Charact.*, 2015, **32**, 72-79.

S4. D. Gopalakrishnan, D. Damien and M. M. Shaijumon, *ACS Nano*, 2014, **8**, 5297-5303.

S5. Y. Wang and Y. Ni, *Anal. Chem.*, 2014, **86**, 7463-7470.

S6. S. Tazuke, S. Kurihara, H. Yamaguchi and T. Ikeda, *J. Phys. Chem*, 1987, **91**, 249-251.

S7. J. Li, S. Tang, L. Lu and H. C. Zeng, *J. Am. Chem. Soc.*, 2007, **129**, 9401-9409.